NASA/TM–2021–0022513

Evaluation of Sensor Uncertainty Mitigation Methods for Detect-and-Avoid Systems

Michael Abramson
Senior Engineer, Crown Consulting, Inc., Moffett Field, California, 94035-1000

Mohamad Refai
Senior Engineer, Crown Consulting, Inc., Moffett Field, California, 94035-1000

M. Gilbert Wu
Research Engineer, NASA Ames Research Center, Moffett Field, California, 94035-1000

Seungman Lee
Aerospace Engineer, NASA Ames Research Center, Moffett Field, California, 94035-1000

October 2021

NASA STI Program ... in Profile

Since its founding, NASA has been dedicated to the advancement of aeronautics and space science. The NASA scientific and technical information (STI) program plays a key part in helping NASA maintain this important role.

The NASA STI Program operates under the auspices of the Agency Chief Information Officer. It collects, organizes, provides for archiving, and disseminates NASA's STI. The NASA STI Program provides access to the NASA Aeronautics and Space Database and its public interface, the NASA Technical Report Server, thus providing one of the largest collection of aeronautical and space science STI in the world. Results are published in both non-NASA channels and by NASA in the NASA STI Report Series, which includes the following report types:

- TECHNICAL PUBLICATION. Reports of completed research or a major significant phase of research that present the results of NASA programs and include extensive data or theoretical analysis. Includes compilations of significant scientific and technical data and information deemed to be of continuing reference value. NASA counterpart of peer-reviewed formal professional papers, but having less stringent limitations on manuscript length and extent of graphic presentations.

- TECHNICAL MEMORANDUM. Scientific and technical findings that are preliminary or of specialized interest, e.g., quick release reports, working papers, and bibliographies that contain minimal annotation. Does not contain extensive analysis.

- CONTRACTOR REPORT. Scientific and technical findings by NASA-sponsored contractors and grantees.

- CONFERENCE PUBLICATION. Collected papers from scientific and technical conferences, symposia, seminars, or other meetings sponsored or co-sponsored by NASA.

- SPECIAL PUBLICATION. Scientific, technical, or historical information from NASA programs, projects, and missions, often concerned with subjects having substantial public interest.

- TECHNICAL TRANSLATION. English-language translations of foreign scientific and technical material pertinent to NASA's mission.

Specialized services also include creating custom thesauri, building customized databases, and organizing and publishing research results.

For more information about the NASA STI Program, see the following:

- Access the NASA STI program home page at ***http://www.sti.nasa.gov***

- E-mail your question via the Internet to help@sti.nasa.gov

- Fax your question to the NASA STI Help Desk at 443-757-5803

- Phone the NASA STI Help Desk at 443-757-5802

- Write to:
  NASA STI Help Desk
  NASA Center for AeroSpace Information
  7115 Standard Drive
  Hanover, MD 21076–1320

NASA/TM–2021–0022513

Evaluation of Sensor Uncertainty Mitigation Methods for Detect-and-Avoid Systems

Michael Abramson
Senior Engineer, Crown Consulting, Inc., Moffett Field, California, 94035-1000

Mohamad Refai
Senior Engineer, Crown Consulting, Inc., Moffett Field, California, 94035-1000

M. Gilbert Wu
Research Engineer, NASA Ames Research Center, Moffett Field, California, 94035-1000

Seungman Lee
Aerospace Engineer, NASA Ames Research Center, Moffett Field, California, 94035-1000

National Aeronautics and
Space Administration

Ames Research Center
Moffett Field, California, 94035-1000

October 2021

Available from:

NASA Center for AeroSpace Information
7115 Standard Drive
Hanover, MD 21076-1320
443-757-5802

Abstract

The impact of sensor noise on the performance of Detect-And-Avoid (DAA) systems can be reduced by implementing various mitigation schemes. This paper evaluates two such methods. One of them is the Sensor Uncertainty Mitigation (SUM) method, implemented in the Detect and Avoid Alerting Logic for Unmanned Systems (DAIDALUS) algorithm, a reference implementation in the DAA minimum operational performance standards. The second method is the Virtual Intruder State Aggregation (VISA), which averages multiple subsequent intruder states extrapolated to the current (most recent) time into a single "aggregated" intruder state. The VISA method can be used either individually as a sensor noise mitigation method in its own right, or in combination with DAIDALUS SUM. The performance of these methods is evaluated using three safety and operational suitability metrics and compared with a baseline configuration using static safety buffers. A large number of encounters representative of low-speed unmanned aircraft against non-cooperative manned aircraft, not equipped with a broadcasting transponder or ADS-B out system, are simulated and evaluated. An air-to-air radar model produces representative sensor noise for the DAA system. Results show that increasing the DAIDALUS SUM parameters for horizontal and vertical uncertainty improves the safety metric at the cost of increasing the number of actionable alerts leading to increased workload. A range of SUM parameters is recommended as suitable values for the type of operations considered for this work. VISA was found to be almost as effective as other noise mitigation methods even when it was used alone. Combining VISA with DAIDALUS SUM achieved the best performance among all investigated methods used with DAIDALUS. General trends and optimal SUM configurations were found to be nearly the same for two large and very different encounter data sets.

Contents

Nomenclature

ADS-B	Automatic Dependent Surveillance – Broadcast
AST	active surveillance transponder
ATAR	air-to-air radar
ATC	Air Traffic Control
CPA	closest point of approach
CPDS	Conflict Prediction and Display System
DAA	detect-and-avoid
DAIDALUS	Detect and Avoid Alerting Logic for Unmanned Systems
DWC	DAA Well Clear
FOV	field of view
GPS	Global Positioning System
GRACE	Generic Resolution Advisor and Conflict Evaluator
h*	vertical separation threshold
HITL	human-in-the-Loop
HMD*	horizontal miss distance threshold
JADEM	Java Architecture for DAA Extensibility and Modeling
LoDWC	loss of DAA well clear
MATG	Multimodal Adaptable Trajectory Generator
MOPS	Minimum Operational Performance Standards
NAS	National Airspace System
SLoWC	severity of loss of Well Clear
SUM	Sensor Uncertainty Mitigation
SWaP	size, weight, and power
UA	unmanned aircraft
UAS	unmanned aircraft systems
VFR	visual flight rules
VISA	Virtual Intruder State Aggregation
WCR	Well Clear Recovery
N_{pa}	number of pilot action count per encounter
S	weighted average performance index over all metrics
s_k	performance index for k^{th} metric
$t_{\text{WCR-LoDWC}}$	average time between unmitigated WCR and LoDWC

1 Introduction

Successful integration of Unmanned Aircraft Systems (UAS) into the National Airspace System (NAS) is predicated upon maintaining or exceeding the level of safety and performance achieved by current operations [3]. RTCA Special Committee 228 (SC-228) is developing UAS Minimum Operational Performance Standards (MOPS) to achieve this goal. These DAA MOPS define the Detect-And-Avoid function [25], which comprises three sub-functions, namely, detection, alerting, and guidance. In addition, the DAA MOPS [26] introduce an algebraic definition of what it means to be Well Clear of other aircraft, referenced hereinafter as DAA Well Clear (DWC) (see Section 2).

The DAA Detect function uses onboard or ground surveillance systems to detect traffic. Of particular relevance is the ability to detect non-cooperative traffic, such as aircraft that do not have a broadcasting transponder or ADS-B system. The DAA MOPS require an onboard air-to-air radar (ATAR) for this purpose (see [24] for ATAR requirements). The Alerting and Guidance functions provide notification of potential hazards that may arise with detected aircraft, and the solutions available to avoid or mitigate observed hazards.

One of the key challenges in implementing effective DAA systems, is sensor noise. The effects of sensor noise are varied and may include degraded alerting and guidance stability. Alerting, for example, may flicker, randomly flashing on and off or changing between different severity levels. Maneuver guidance may also exhibit distracting fluctuations. This can be detrimental to effective mitigation of hazards for both pilot-in-control concept of operation, which is adopted in the DAA MOPS, and fully automated DAA. Furthermore, different sensor systems may exhibit distinctly different noise characteristics. For example, ATAR detects bearing of another aircraft (an intruder) relative to the UA controlled by the UAS pilot (ownship) with an order of magnitude better accuracy than a mode-C transponder.

It is therefore desirable for DAA systems to take sensor noise characteristics into account.

Several schemes for mitigating the effects of noise are possible. One approach is to provide correlated smoothed intruder states [6, 13, 16, 23, 31–34], which are then used to predict hazards. This is commonly done using a tracker. Any residual noise that exists after track processing can be further reduced using Virtual Intruder State Aggregation (VISA) described in this paper.

Another approach to sensor noise mitigation allocates a buffer to inflate desired separation thresholds, thus providing more conservative hazard predictions [15].

Other approaches modify the raw alert sequence by imposing alerting persistence requirements and/or delaying the onset of an alert until a certain number of hazards are reported in a given period of time for each intruder [25]. These methods and others are not mutually exclusive and may be used in combination to achieve desired DAA performance.

Our previous paper [5] investigated the benefits of using sensor uncertainty information in a Sensor Uncertainty Mitigation (SUM) method, which was implemented in the Detect and Avoid Alerting Logic for Unmanned Systems (DAIDALUS), the reference algorithm adopted in the DAA MOPS. DAIDALUS SUM performance was compared with separation buffers using the same safety and operational suitability metrics. Closed loop DAA simulations incorporating UAS pilot resolutions were used, with SUM parameters being the independent variables. Open loop alerting-only simulations were also used to assess open-loop alerting metrics.

This paper extends the previous research [5] by adding results for other SUM parameters and by investigating the benefits of smoothed (aggregated) intruder states using the VISA method, either individually as a sensor noise mitigation method in its own right, or in combination with DAIDALUS SUM.

The paper is organized as follows. The next section provides a high-level background on DAA systems. Section 3 provides an overview of previous work related to sensor uncertainty mitigation methods. Section 4 describes the approach used to evaluate SUM performance. Section 5 describes the main results. Finally, concluding remarks are presented in Section 6.

2 Background on Detect-and-Avoid

The DAA system assists UAS operators and pilots in maintaining separation with other aircraft. One of the core challenges of such capability is to meet the Federal Aviation Administration (FAA) requirements to "see and avoid" and when passing other aircraft to remain "well clear" as mandated for manned aircraft in 14 CFR §91.113 [1]. UAS pilots are not in the flight deck to "see and avoid," so pilots must rely on surveillance and algorithms for conflict detection and avoidance. In this situation, the separation standard, referred thereafter as DAA Well Clear (DWC), must be defined quantitatively. To provide information for maintaining DWC, the DAA system computes alerts and maneuver guidance based on a look-ahead time of 1 to 2 minutes. The alerting and maneuver guidance structure in the DAA MOPS is designed with the assumptions that a UAS flies by instrument flight rules (IFR) and UAS operators or pilots are "in the loop" using DAA as the primary means of separation between the UAS and surrounding VFR flights. Air Traffic Control (ATC) is primarily responsible for separation between the UAS and surrounding IFR flights. IFR requires pilots to contact ATC for a DAA maneuver if they have enough time to ask for ATC guidance. Otherwise pilots evaluate the situation and choose an appropriate maneuver with the aid of the DAA system. Finally, pilots enter a maneuver manually for execution by aircraft. All these operations contribute to the pilot response delay. Ground-air communication latency can cause additional delay, which was not considered in this study.

The study applies a DWC that is to be defined in an upcoming revision of the DAA MOPS [26] for en-route encounters with non-cooperative intruders, i.e., VFR aircraft without a broadcasting transponder or ADS-B out system. Encounters with non-cooperative intruders pose unique challenges because of sensor noise and especially large vertical state uncertainty typical for ATAR. This study focuses on the DAA system's performance against non-cooperative intruders in an operational environment representative of UAS with low size, weight, and power (SWaP) sensors, i.e., low speed unmanned aircraft (UA) and a limited surveillance range (see Subsection 4.3 for more details). The DWC for a non-cooperative intruder is a short cylinder (a "hockey puck") with a horizontal radius of 2,200 ft and a vertical threshold of 450 ft above and below the UA [30].

The DAA MOPS define three types of alerts in increasing levels of severity: preventive, corrective, and warning. The corrective alert indicates that a loss of DAA well clear (LoDWC) is predicted to occur in the future, an avoidance maneuver is necessary, but there is still time for coordination with air traffic control (ATC). The warning alert indicates that a LoDWC is imminent, an avoidance maneuver is needed, and coordination with ATC before maneuvering is not a requirement. The preventive alert effectively has the same thresholds and alerting times as a corrective alert, but with larger vertical separation between 450 to 700 feet. The DAA system should not issue preventive alerts for non-cooperative aircraft due to the lack of precise altitude information. Therefore, preventive alerts are not modeled in this study.

The DAA system must present maneuver guidance to UAS pilots in the form of DWC-based, conflict-free aircraft headings or altitude ranges, or "bands." In case a LoDWC is imminent, these bands become "saturated," meaning there are no conflict free headings or altitudes and that a loss of DWC is unavoidable no matter what action a UAS pilot takes. In this case the DAA system should present Well Clear Recovery (WCR) guidance. This is a range of headings or altitudes that, if executed, can increase separation at CPA and regain DWC effectively. Figure 1 depicts a mockup of guidance to remain and regain DWC. In this figure red (warning) or yellow (corrective) represent the ranges of headings or altitudes that will result in a LoDWC, and green depicts the guidance that will (a) avoid a LoDWC or (b) effectively regain DWC.

(a) Guidance to Remain Well Clear

(b) Guidance to Regain Well Clear

Figure 1: Guidance Display Examples

Several alerting and guidance algorithms have been developed to support research, development, and evaluation of DAA MOPS. One of the first such algorithms was implemented in General Atomics' Conflict Prediction and Display System (CPDS) that included a UAS pilot display with conflict probing [27]. CPDS was extensively tested in flight tests with NASA's Ikhana UAS vehicle, a variant of MQ-9.

NASA developed the Generic Resolution Advisor and Conflict Evaluator (GRACE), which combined flexibility, robustness, and computational efficiency [4]. GRACE provided the core alerting and guidance functions of NASA's Java Architecture for DAA Extensibility and Modeling (JADEM) system [4]. GRACE was used in a number of real-time and fast-time experiments, including parametric studies, NAS-wide simulations, human-in-the-loop experiments, and live flight tests.

Another alerting and guidance algorithm, DAIDALUS [19], was developed by NASA specifically to support Phase 1 DAA MOPS [25] and is integrated in JADEM software alongside with other DAA algorithms [4]. DAIDALUS uses closed-form solutions to compute alerts for the ownship and the intruders, and suggestive guidance in the form of heading or altitude "bands," i.e., ranges of ownship maneuvers.

The recently developed Aircraft Collision Avoidance System X (ACAS-X) [21] is envisioned by the FAA as a replacement for the currently deployed Traffic Alert and Collision Avoidance System II (TCAS-II) [2]. The UAS-variant of ACAS-X, called ACAS-Xu, is being developed to meet the DAA requirements defined by the SC-228 in DO-365 [25].

3 Sensor Uncertainty Mitigation Methods

3.1 Input State Stability

The first "line of defense" against sensor noise is improving stability of input states for DAA algorithms. This can be done using multi-state filtering and estimation methods that are usually considered in the context of surveillance tracking and fusion algorithms [6, 13, 23, 31, 33]. One of the earliest and simplest techniques was an alpha-beta filter that assumed fixed covariance errors and a constant-speed target model to update tracks [16]. The most widely used probabilistic filters are Kalman (KF) and Extended Kalman Filters (EKF) [32]. These filters are error-prone and have quadratic complexity that can be reduced by various modifications and upgrades, such as Compressed EKF, Information Filter or Extended Information Filter, Sparse Extended Information Filter, Divide and Conquer, or Conditionally Independent Submaps [23]. Particle Filtering

(PF) [18] is becoming an increasingly popular alternative to KF and EKF. It can be difficult, however, to define a sufficient number of particles (samples) for a correct calculation [23]. Even more sophisticated filtering and estimation methods, such as the Interacting Multiple Model (IMM) [31] and Multiple Hypothesis Tracking (MHT) [34] algorithms, have been proposed. These methods, in various combinations with other algorithms, can be especially useful for multiple targets with unpredictable movements.

Ideally, if surveillance used with low SWaP DAA systems were to implement high-quality fusion trackers using the appropriate filtering methods listed above, it might prove sufficient to ensure adequate performance of deterministic state-based algorithms, such as DAIDALUS. However, simulation results demonstrated that even DAIDALUS with SUM was not always able to compensate for residual noise from a tracker [12]. Therefore, multi-state filtering techniques can be useful alternative or additional noise mitigation methods.

JADEM currently supports EKF and a family of methods based on the idea of "virtual intruders," generated by extrapolation of several past intruder states from tracker output to the current (most recent) time t_n. The simplest method in this family, Virtual Intruder State Aggregation (VISA), averages all these extrapolated states, shown as black vectors for time t_n in Figure 2, into a single "aggregated" intruder state, shown as a bold blue vector.

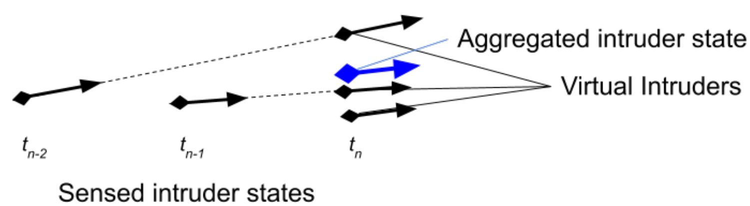

Figure 2: Virtual Intruder State Aggregation for three consecutive states

Conceptually this method is similar to a special case of alpha-beta filter, known as the alpha-filter [16].

3.2 Static Buffers

A traditional approach to mitigating sensor noise and other sources of uncertainty in aircraft states involves adding spatial or temporal safety buffers. An example of such an approach for UAS DAA systems can be found in [15]. GRACE and DAIDALUS both support user-defined safety buffers by allowing multiple "nested" separation standards.

This method is simple and effective, but it involves trade-offs in performance. Large safety buffers may increase the likelihood of incorrect alerts defined in DAA MOPS as alerts issued when the intruder aircraft remains in the Non-Hazard Zone, where the DAA MOPS defines that the DAA system must not alert [25]. This can lead to unnecessary maneuvers, therefore increasing workload. Moreover, one static buffer that works for intruders detected by a certain sensor may not work well for intruders detected by a different sensor due to variation of sensor uncertainty characteristics.

3.3 Alert Stability

The DAA MOPS include an alert hysteresis requirement, which aims to reduce undesired alert flickering [25]. The requirement is that an alert "shall persist for a minimum of four seconds, unless the intruder is declared a higher priority alert." In addition, the DAA MOPS also suggest the use of an M-of-N ($M < N$) alert filter, which requires that an alert must be present in at least M of N consecutive detection cycles, in order for the alert to be valid. The effect is to delay alerting and guidance displayed to the UAS pilot until the alerts have sufficiently stabilized. This helps a PIC to act more confidently and to avoid excessive or unnecessary maneuvering based on misleading alerts. JADEM supports both persistence and M of N alerting logic that can be enabled no matter which DAA algorithm is used.

3.4 Guidance Stability

The use of hysteresis or M of N, however, cannot mitigate gradual changes in alerts caused by low-frequency components of tracker noise, or by maneuvering aircraft, or both. Furthermore, they do not address the issue of guidance fluctuations, which may confuse a UAS pilot or lead to erroneous maneuvers. One approach to addressing this issue would be to apply persistence logic for guidance in the same way as it was used for alerts. The persistence logic should also prevent too frequent changes in guidance information. The effectiveness of this method has not yet been rigorously evaluated.

Some DAA algorithms, such as GRACE, can use the intent information about ownship and intruders to generate more accurate predictions that are used for guidance. In principle, this could provide the adequate mitigation for slow alerting changes caused by maneuvers, assuming that the intent information is correct. However, the intent of non-cooperative intruders is not known, and even if it were known, the DAA MOPS-compliant algorithms are not required to take it into account. In addition, intent information will not help if maneuvering aircraft are not the cause of low-frequency tracker noise in a given encounter.

A more reliable way to suppress abrupt guidance changes is to use a cost/reward function that allows a flexible balance between guidance stability and other considerations. This approach is used by both GRACE and ACAS algorithms that demonstrated robust performance under simulated sensor uncertainties [4,10]. GRACE was tested in simulations with a model of noisy airborne radar and it was able to resolve all conflicts unless they were detected too late because of the limited sensor's field of regard [4]. ACAS-Xu was compared with DAIDALUS using flight test data flown with scripted encounters and was found to be more resilient [10].

3.5 DAIDALUS SUM

If sensor uncertainty information is available in real time, it can be used to improve alerting and guidance stability. For instance, ACAS-Xu utilizes this information in computation of its "belief states" representing estimated relative positions of other aircraft [9]. The Sensor Uncertainty Mitigation (SUM) capability, recently added to DAIDALUS, also follows a similar approach.

DAIDALUS SUM uses sensor uncertainty information to compute bounds on the errors in the aircraft position and velocity vectors [20]. These bounds are used to create "phantom" intruders, which are then used to compute alerting and guidance by combining the results for each phantom with those for the sensed intruder as shown in Figure 3. This approach is effectively creating a "dynamic" buffer, which is reevaluated with every detection cycle.

SUM requires six tunable parameters. Three of these parameters are z-scores indicating the number of standard deviations to consider for horizontal and vertical position uncertainty and for vertical velocity uncertainty:

h_pos_z   number of standard deviations for horizontal position uncertainty
v_pos_z   number of standard deviations for vertical position uncertainty
v_vel_z   number of standard deviations for vertical velocity uncertainty

The other three tunable parameters for horizontal velocity uncertainty are:

h_vel_z_score_min   number of standard deviations for horizontal velocity uncertainty at high distance
h_vel_z_score_max   number of standard deviations for horizontal velocity uncertainty at low distance
h_vel_z_distance   distance at which to start phasing between the high distance and low distance values

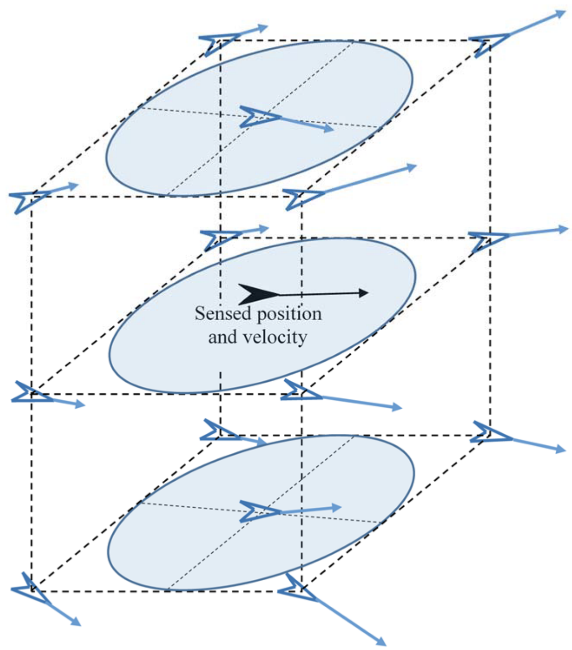

Figure 3: Phantom Intruders in DAIDALUS SUM

The use of the last three parameters requires some clarification. SUM provides the option to use a smaller velocity uncertainty when the aircraft are further apart because a slight change in the size of the velocity error at those distances can produce a very large set of possible future states as those velocities are propagated in time. This problem is mitigated by allowing the horizontal velocity uncertainty, expressed as a number of standard deviations, to decrease as the aircraft get further apart.

For a given level of sensor noise, larger z-scores by definition have the effect of increased "dynamic buffers" around a "sensed" intruder. Larger z-scores are therefore expected to make alerts and bands more stable. At the same time, alerts may be issued earlier, and the probability of incorrect alerts may increase. Furthermore, using large z-scores may result in wider bands that may become saturated earlier than necessary. Increasing z-scores will therefore result in increasingly conservative guidance, which may cause pilots to use more aggressive or excessive maneuvers.

Evaluation of an earlier version of SUM using a limited number of encounters (as defined in subsection 4.3) was conducted in [11, 12, 14]. The main alerting metric used for evaluation was Alert Jitter, which is defined as the average number of transitions to alerts of higher severity (e.g. from corrective to warning alerts) that occur within an encounter set. The effectiveness of guidance was evaluated using Severity of Loss of Well Clear (SLoWC) metric, capturing the most serious instance of LoDWC throughout an encounter. SLoWC ranges from 0% (DAA Well Clear maintained throughout the encounter) to 100% (mid-air collision). Results showed improvement in alert stability and safety metrics with SUM. However, the tunable SUM parameters in all these studies varied only within narrow ranges. Also, the small number of encounters simulated (< 300) was not enough for accurate estimates of safety metrics such as the SLoWC. Moreover, the optimal values of these parameters may be very different if more metrics are used and if Phase 2 requirements for aircraft and sensor performance are assumed. The key objective of the Phase 2 work at SC-228 is the use of low SWaP sensors. This implies several other requirements, such as lower aircraft speeds, faster turn rates, and shorter radar range. The need to find the most suitable values of SUM parameters for Phase 2 DAA MOPS motivated this study.

4 Approach

4.1 Simulation Architecture

The simulations in this study are conducted using JADEM, developed by NASA to support evaluation of different DAA concepts and their safety characteristics [4]. Figure 4 depicts the simulation architecture used. The components in the figure are described in more detail in subsections 4.4–4.7 below.

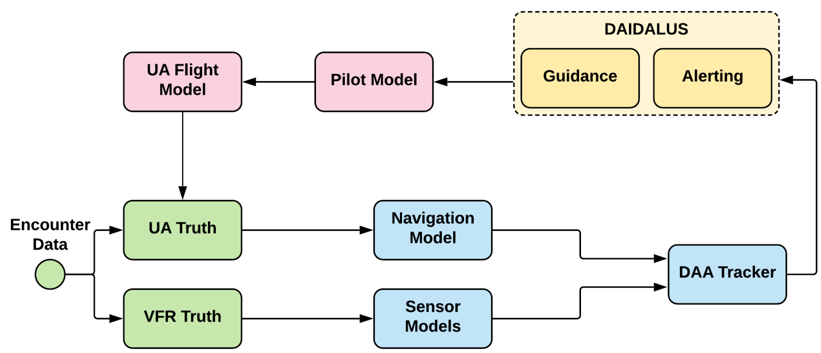

Figure 4: Simulation Architecture

4.2 Metrics

Three metrics are analyzed in this study:

1. SLoWC ratio, defined as the ratio of averages of SLoWC between mitigated and unmitigated runs for the same encounter set and configuration. The advantage of this metric is that it captures not only the number of LoDWC events, but also how "severe" (i.e. close to NMAC) these events were. A value of zero for a specific encounter means that there was no loss of DWC during that encounter. So an increase in the average SLoWC value across all encounters either means that the LoDWC that occurred were more severe because aircraft were closer to each other, or that there were more LoDWC in the encounter set. Therefore, the lower value

of SLoWC ratio indicates that the UAS pilot is more successful in avoiding the LoDWC, and if the losses of DWC cannot be avoided, the pilot maneuvers make them less serious.

2. Number of UAS pilot actions (i.e. evaluation and execution of maneuvers) per encounter, denoted as N_{pa}. This metric can be used to characterize the workload. It also may have implications for safety due to the factors that are not captured by the DAA pilot model used in this study. For instance, more conservative guidance may have an effect on UAS pilot fatigue and decision-making capabilities.

3. Average time between the time when well clear recovery (WCR) guidance first displayed to a pilot and the time of LoDWC, denoted as $t_{\text{WCR-LoDWC}}$. Any non-negative WCR-to-LoDWC time is considered acceptable by the DAA MOPS. However, for operational reasons $t_{\text{WCR-LoDWC}}$ should not be too large because WCR presents a risky situation in which pilots are given limited guidance, which should not be displayed earlier than necessary. Since the maneuver time needed to resolve a conflict is typically from 10 to 20 seconds [25], it is assumed that WCR to LoDWC time should not exceed 20 seconds.

4.3 Encounters

For our purposes, we define pairwise encounters as trajectory portions from one ownship and one intruder that can potentially cause loss of well clear or alert with the ownship or peripheral guidance computed by DAIDALUS [19]. The study used more than 80,000 pairwise encounters generated from a subset of projected UAS mission profiles developed under prior work [7] that represent low SWaP UAS, and recorded radar traffic data that include visual flight rules and non-cooperative flights [22]. The encounters have the following properties when the aircraft are at their closest point of approach (CPA):

- ownship's true airspeed is between 40 and 110 KTAS.
- intruder's true airspeed is below 170 KTAS, a 95 percentile upper bound for non-cooperative aircraft [17].
- ownship's altitude is below 11000 feet MSL.

More details about the encounters can be found in [29].

4.4 Sensor and Tracker Models

For this study, the intruders' simulated trajectory states, referred hereafter as "truth" states, were perturbed by a radar model with a vertically cylindrical radar field of view (FOV) with a radius of 3 NM, representative of the range of a low SWaP radar. Analysis with this type of FOV sheds light on the sensitivity of the DAA performance metrics to a finite surveillance range, a critical question for UAS operations with low SWaP sensors. Representative values used for azimuth and elevation errors were $0.5^\circ \pm 1.0^\circ$ and those for (slant) range error were 15 ± 21 meters. The Phase 1 MOPS require a tracker that fuses and correlates measurements from multiple sensors for a single intruder into tracks. The UA's state is also input into the tracker to produce the intruder's state in absolute coordinates. A fusion tracker developed by Honeywell [8] is used for this work. This tracker outputs the intruder's track position and velocity as well as their estimated accuracies.

4.5 Alerting and Guidance Algorithm

For this study, DAIDALUS is configured to issue a corrective alert 60 seconds and a warning alert 30 seconds before the UA is predicted to enter the alert conflict zone based on the DWC. Upon alerting, DAIDALUS generates corresponding preventive, corrective, and warning guidance indicating a range of conflict-free headings and altitudes for the UAS pilot to select from in order to maintain DWC separation. In the absence of alerts, DAIDALUS still computes peripheral guidance by projecting candidate vertical and horizontal DAA maneuvers into future times to determine which would result in conflicts. DAIDALUS also computes regain DWC guidance, known also as well clear recovery (WCR), if a LoDWC is unavoidable.

For simulations with a static buffer, the DWC's horizontal radius, or the horizontal miss distance threshold (HMD*) is scaled by a factor of 1.52 to be consistent with the parameters referenced in the Phase 1 DAA MOPS. In one configuration with static buffer the vertical threshold, h*, was set to 450 ft value that was defined as the vertical threshold of the DWC in the DAA MOPS. In another configuration h* is set to 4000 ft, which is the value of a conservative threshold suggested by the DAA MOPS to guard against the large vertical state noise of an ATAR detecting non-cooperative aircraft. All runs with DAIDALUS SUM use the unbuffered HMD* = 2200 ft and vertical threshold h* = 450 ft.

4.6 Pilot Response Model

The DAA MOPS reference pilot response model calibrated from UAS pilot performance data obtained in the Human-in-the-Loop (HITL) simulations [29] was used to select maneuvers from DAA guidance and execute them. Appropriate delays at various states are applied to mimic the air traffic coordination time and pilot evaluation time. The initial 5-second delay represents the time it takes the pilot to perceive the alert and devise a plan. For corrective alerts, an additional 11 second ATC coordination time elapses, representing the time the pilot spends to communicate the intended maneuver with ATC and receive approval. The model then follows with a 3-second execution delay representing the time it takes the pilot to enter a maneuver command into the control station and transmit this command to the UAS. More details are described in [29]. Only horizontal maneuvers are used because large vertical state errors for non-cooperative intruders make vertical maneuvers less robust.

4.7 UA Flight Model

Once the UAS pilot response model selects a DAA maneuver and the execution delay elapses, the flight model takes control and modifies the UA's truth trajectory in accordance with the DAA maneuver. JADEM's flight model is based on Multimodal Adaptable Trajectory Generator (MATG) [4], a fast and flexible kinematic trajectory predictor. MATG can handle any constraints (position, heading, speed, altitude, vertical speed, and time) in any combination. The UA kinematics can be modeled using either bank angle or turn rate and vertical speeds that can be defined as functions of altitude and flight phase (climb/descent). When MATG is used for modeling pilot maneuvers, the target heading or altitude constraint is created from the output of the DAA pilot model. Once the flight model has achieved the target heading or altitude, the UA trajectory retains it until the end of the encounter. The intruder's trajectories may include heading or altitude changes, but they are not affected by ownship maneuvers.

In this study, the DAA pilot model selected only heading guidance, and a constant turn rate of

7 deg/sec was assumed for all UA maneuvers, which is consistent with the Low-SWaP performance parameters suggested in the Phase 2 DAA MOPS. Furthermore, although JADEM allows the specification of wind magnitude and direction, no wind was assumed in modeling aircraft maneuvers.

4.8 Experiment Setup

Evaluating the effectiveness of sensor uncertainty mitigation necessitates comparisons between the following scenario configurations:

1. *Perfect*: the baseline case with "perfect" surveillance data without simulated sensor errors but with limited FoV representative of low SWaP airborne radar.
2. *Noisy*: similar to the perfect case but uses the sensor and tracker model developed by Honeywell [8], for airborne radar with the same FoV.
3. *Mitigated*: similar to the noisy case but configured to use one or more noise mitigation methods, such as static buffers, VISA, or DAIDALUS SUM with different tunable parameters.

Perfect, noisy, and each of the mitigated configurations required two runs: "open loop," which was used to generate metrics without executing avoidance maneuvers, and "closed loop" with aircraft maneuvering in accordance with the UAS pilot response model (see Section 4.6 for more details).

This section presents results for the following *Mitigated* configurations, compared with *Perfect* and *Noisy* configurations as defined in 4.8:

1. **HMD* buffer**: the HMD threshold was set to 3342 ft, replacing the standard 2200 ft HMD threshold, using the same scaling factor 1.519 (from 4000 ft to 1 nmi) that the DAIDALUS team used for their reference configuration file for the cooperative DWC [26].
2. **HMD* & Vert. buffer**: in addition to the HMD* buffer, the vertical threshold was set to 4000 ft, to protect against large radar errors in vertical state.
3. **SUM**: DAIDALUS SUM with different combinations of horizontal and vertical tunable parameters.
4. **VISA**: the VISA was used as the only sensor noise mitigation method with DAIDALUS running without static buffers and SUM. VISA was averaging 5 subsequent intruder states that provided a good trade-off between smoothness of VISA output and delays in alerts that would increase if more intruder states were used.
5. **VISA & SUM**: the VISA used in combination with DAIDALUS SUM.

For most of **SUM** configurations, the following assumptions were made for SUM parameters:

- h_vel_z_score_max = h_pos_z
- h_vel_z_distance = 3.0 nmi
- h_vel_z_score_max / h_vel_z_score_min = 5
- v_vel_z = v_pos_z

This leaves only two independently varying parameters to generate a 2D map of performance metrics for **SUM** configurations: horizontal and vertical position z_scores.

In addition to these configurations, a few additional variations of SUM parameters were evaluated to determine whether SUM performance could be further improved.

4.9 Performance Evaluation

This study attempts to compare the overall performance of each simulation configuration via a single cost function by combining the aforementioned three metrics defined in Subsection 4.2. This approach is generally challenging and subjective. Nonetheless, this attempt will demonstrate the trade space between metrics and determine a reasonable range of SUM parameters.

To facilitate the construction of this cost function, the performance indices s_k were calculated for all metrics. The lower values of these indices always indicate the better performance. For the first two metrics, SLoWC ratio and N_{pa}, s_k was defined simply as the ratio of value of k^{th} metric for given configuration, denoted as m_k, to its value $m_{k,noisy}$ for *Noisy* configuration:

$$s_k = \frac{m_k}{m_{k,noisy}}, k = 1, 2 \tag{1}$$

The *Noisy* configuration is used as the denominator because this is the case without mitigation that can be used as a natural reference.

The last metric, $t_{\text{WCR-LoDWC}}$, couldn't be normalized the same way since it represented a penalty applied only for a time exceeding a 20 second limit. Hence, its s_k was calculated as:

$$s_k = \frac{max(m_k - m_{k,limit}, 0)}{0.1 * m_{k,limit}}, k = 3 \tag{2}$$

This ensured that s_k was zero when the m_k is below the 20 second limit $m_{k,limit}$, and it rapidly increased once the m_k exceeded $m_{k,limit}$.

The overall performance index S for each configuration was calculated simply by averaging s_k for all metrics with weights w_k reflecting the relative importance of each metric.

$$S = \sum_k w_k s_k \tag{3}$$

This allowed a comparison of overall performance across configurations. Section 5 provides a summary of evaluation results.

5 Results

The results for statistical metrics for buffered and SUM configurations in this section are shown as bar charts with error bars.

5.1 Static Buffers and DAIDALUS SUM

Figure 5 shows the LoWC Severity ratio for different mitigation methods compared to the unmitigated noisy configuration. The left half graph shows results for perfect and unmitigated noisy configurations and for two configurations using static buffers. The right half graph shows results for different SUM configurations. Even for perfect configuration, the LoWC severity ratio is not zero because even with accurate information about intruder states, the losses of DWC could not always be avoided when intruders maneuvered unexpectedly. The LoWC Severity ratio for unmitigated noisy configuration is at the level of 16%, more than two times higher than for perfect configuration. This level of LoWC Severity ratio for the worst case of noisy surveillance without any mitigation is high and unlikely to be operationally acceptable. All mitigation methods substantially reduce the LoWC Severity ratio compared to the unmitigated noisy configuration. The

HMD* buffer reduces the LoWC Severity ratio two times, from 16.2% to 8.01%, and the combined HMD* and vertical buffer reduces it even further to 6.5%, comparable with best results for SUM. SUM results show a clear trend of reducing LoWC Severity ratio for increasing horizontal and vertical z_scores. The lowest SLoWC ratios are achieved at horizontal position z_score above 3 and vertical position z_scores 1 or higher, when SUM alerting and guidance become more conservative. Further increase in vertical z_score has little impact because the additional encounters affected by the increasing "dynamic" vertical buffer in SUM have large vertical separation between the aircraft and are unlikely to result in a LoDWC.

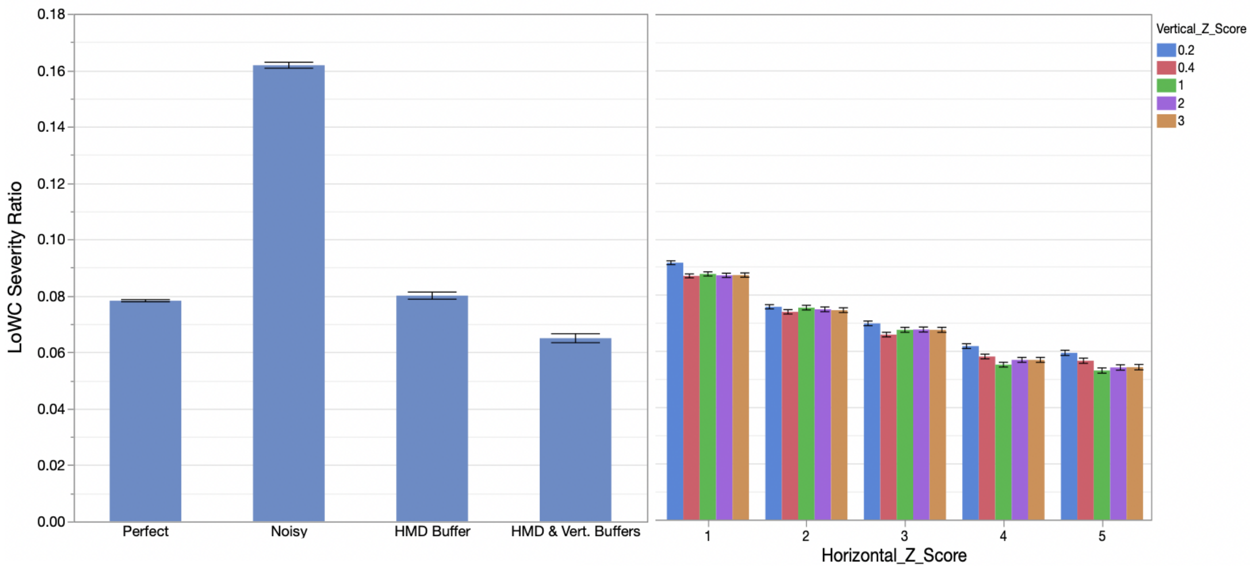

Figure 5: Metrics for LoWC Severity Ratio

The reduction in SLoWC ratios is achieved at the cost of earlier alerts and higher likelihood of incorrect alerts. This results in higher values of N_{pa} as shown in Figure 6. Note that for perfect configuration, N_{pa} is below one because not all encounters require pilot action. All mitigation methods increase N_{pa}, and the most conservative SUM alerting and guidance increases it more than two times compared to noise without mitigation. In other words, pilots may have to work harder to achieve a slightly lower LoWC severity. This increase in workload is expected as was discussed in Subsection 4.2. Note that the vertical buffer and the increase in vertical z_score above 2 have only modest effect.

Figure 7 shows that $t_{\text{WCR-LoDWC}}$ increases more than two-fold when the horizontal static buffer is used, and nearly triples when SUM horizontal z_score increases from 1 to 5. This is a result of early saturation of heading bands, which is a trigger for WCR guidance, for larger horizontal buffers, whether they are static or "dynamic" in SUM. Note that sensor noise by itself has very little effect on band saturation, hence the values of $t_{\text{WCR-LoDWC}}$ for perfect and noisy configurations are similar. More importantly, $t_{\text{WCR-LoDWC}}$ remains below the acceptable 20 second limit only for SUM with horizontal position z_score below 3. This indicates that, irrespective of the trade-off between SLoWC ratio and N_{pa}, using SUM with horizontal z_score higher than 3 will be problematic, since it will allow WCR guidance to appear too early to be operationally suitable.

Since all three metrics tell different stories, it can be helpful to use an overall, or "combined,"

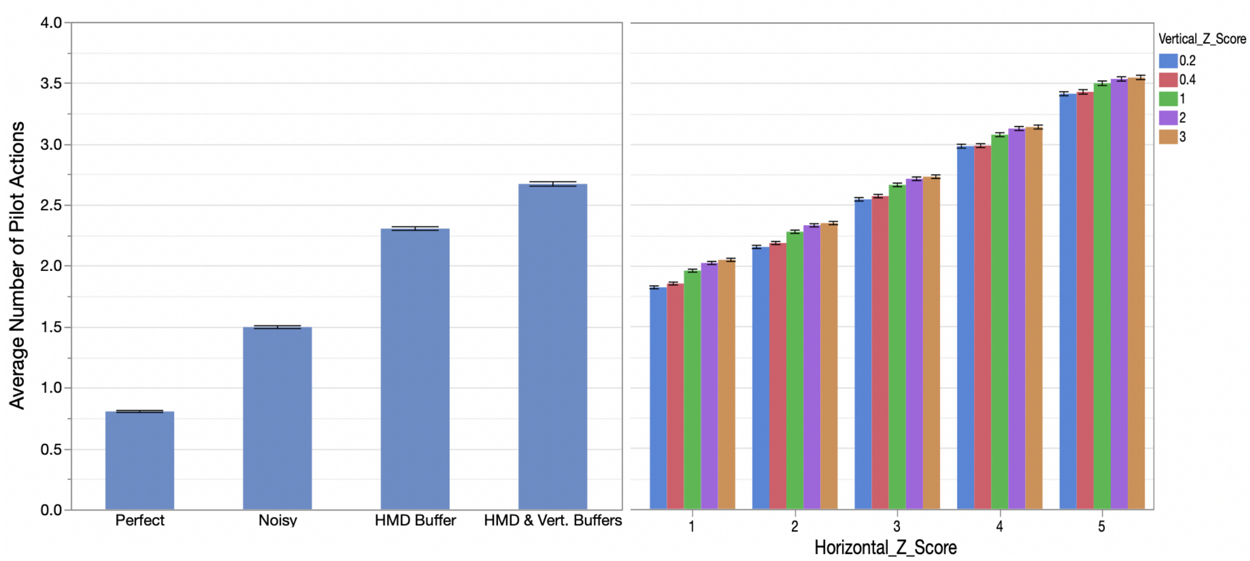

Figure 6: Metrics for N_{pa}

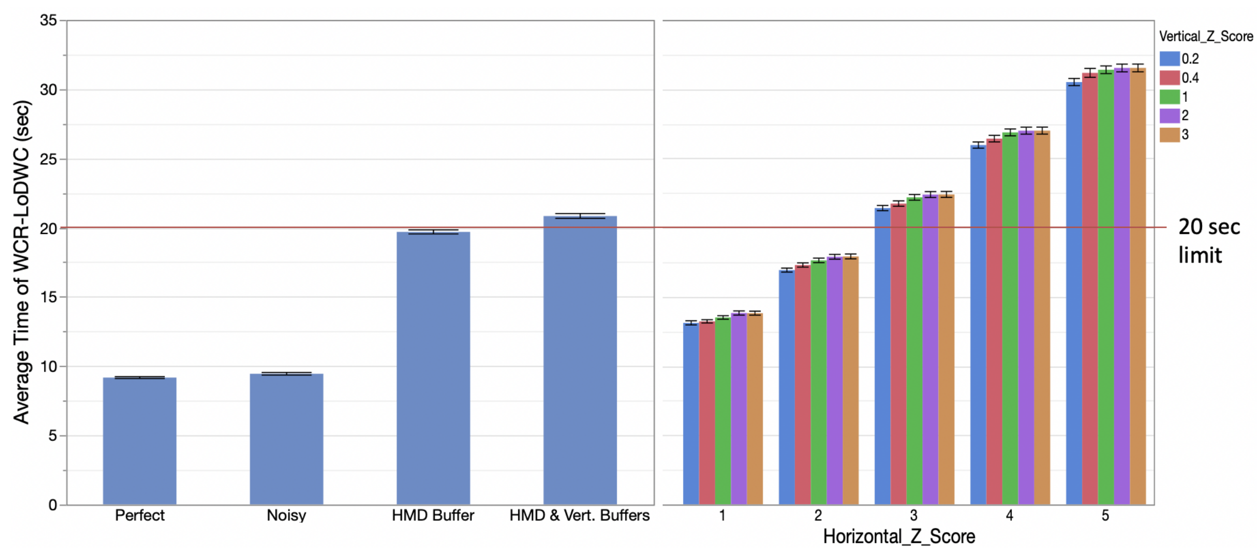

Figure 7: Metrics for $t_{\text{WCR-LoDWC}}$

performance index for each configuration using Equation (3) with particular metric weights. Any choice of these weights is inherently subjective, but for the data in this study it was found that the performance profile for different configurations and the optimal DAIDALUS SUM parameters were insensitive to weights within a wide range of "reasonable" metric weights. Figure 8 illustrates one such choice. Since safety outweighs any operational suitability considerations, the weight of SLoWC ratio w_1 is set to 1 while the weights of N_{pa} and $t_{\text{WCR-LoDWC}}$ are five times lower: $w_2 = w_3 = 0.2$. With this choice, the combined performance index S for each configuration is shown in Figure 8 as a color map with blue and red colors representing the lower (preferred) and the higher values respectively. From this figure it becomes clear that the best mitigation method is SUM with

	buffers		SUM				
	HMD	HMD & vert.	horizontal pos z_score				
	0.570	0.595	1	2	3	4	5
vertical pos z_score 0.2			0.573	0.533	0.645	0.974	1.329
0.4			0.554	0.528	0.652	0.991	1.365
1			0.566	0.542	0.699	1.019	1.373
2			0.569	0.544	0.719	1.039	1.389
3			0.572	0.544	0.720	1.041	1.391

Figure 8: Weighted Average Performance Indices S over All Metrics

the horizontal position z_score equal 2 and vertical position z_score 0.4. The overall combined performance index is less sensitive to the vertical z_score than to the horizontal position z_score.

Configurations with static buffers have slightly higher values of S than the optimal SUM configuration, but they perform better than SUM configurations with horizontal z_score above 2. This may indicate that static buffers used in this study provide a reasonably good approximation for average sensor noise. For sensors with different characteristics the advantage of SUM over static buffers may become more pronounced. Since values of all three metrics are subject to a certain level of error due to the finite number of encounters sampled, all SUM configurations with a horizontal position z_score equal to 2 as well as the HMD* buffer configuration are all considered performing reasonably well.

Relaxing constraints on SUM parameters listed in subsection 4.8 by varying horizontal and vertical velocity scores independently around the best SUM configuration did not lead to finding configurations that would significantly improve overall SUM performance.

Another set of simulations was performed for nearly 200,000 uncorrelated encounters provided by MIT Lincoln Laboratory [28]. General trends and optimal SUM configuration for this larger and very different encounter data set were found to be nearly the same as for NAS-wide encounters that were presented in this section.

5.2 Other DAIDALUS SUM and VISA Configurations

Figures 9 - 12 show the summary of comparisons between perfect, noisy, and buffered noisy configurations on the left side of vertical dividing line against the best SUM configuration denoted as "Noisy SUM," the "DAA MOPS SUM" configuration that was used in Appendix G of [26], and two configurations using VISA. In "Noisy VISA" configuration VISA was the only noise mitigation method. In this case, VISA generated the smoothed intruder states for DAIDALUS, which simply accepted them as its input states and did not use SUM. In "Noisy VISA SUM" configuration VISA was used to generate the intruder input states for DAIDALUS SUM in "Noisy SUM" configuration. All these results were generated for the same 80,000 encounter set described in subsection 4.3. Therefore, Figures 9 - 11 are directly comparable with Figures 5 - 7, and their left sides are identical.

For the LoWC severity Ratio metric, Figure 9 shows that even when VISA was used as the only noise mitigation method ("Noisy VISA" configuration), it reduced the LoWC Severity ratio against the unmitigated "Noisy" configuration. However, all other methods achieved deeper reduction in

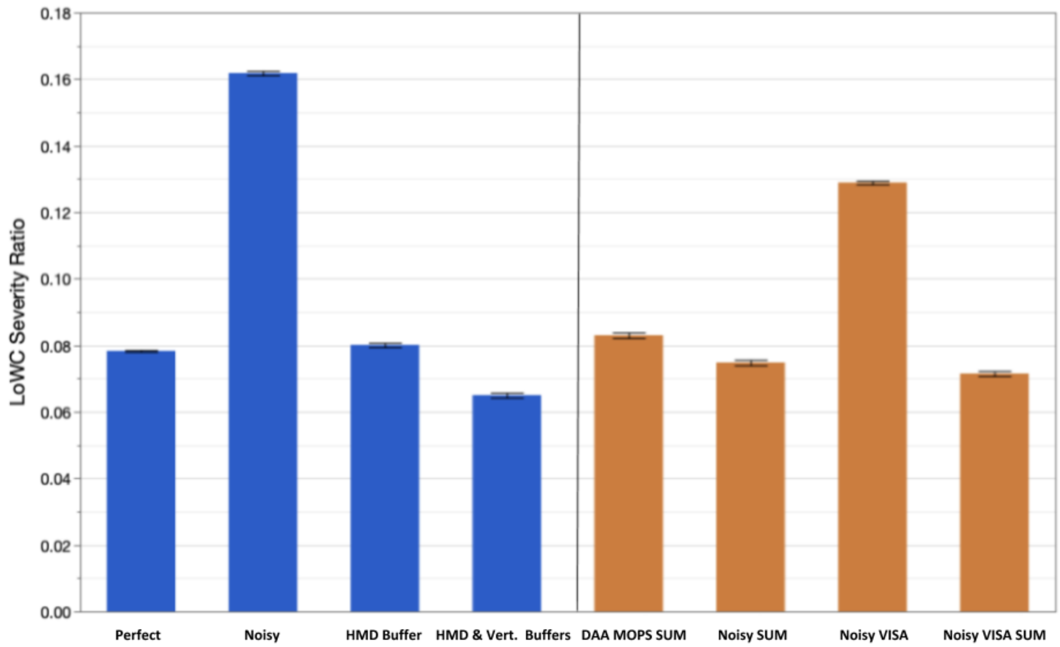

Figure 9: Best SUM and VISA Configurations: LoWC Severity Ratio

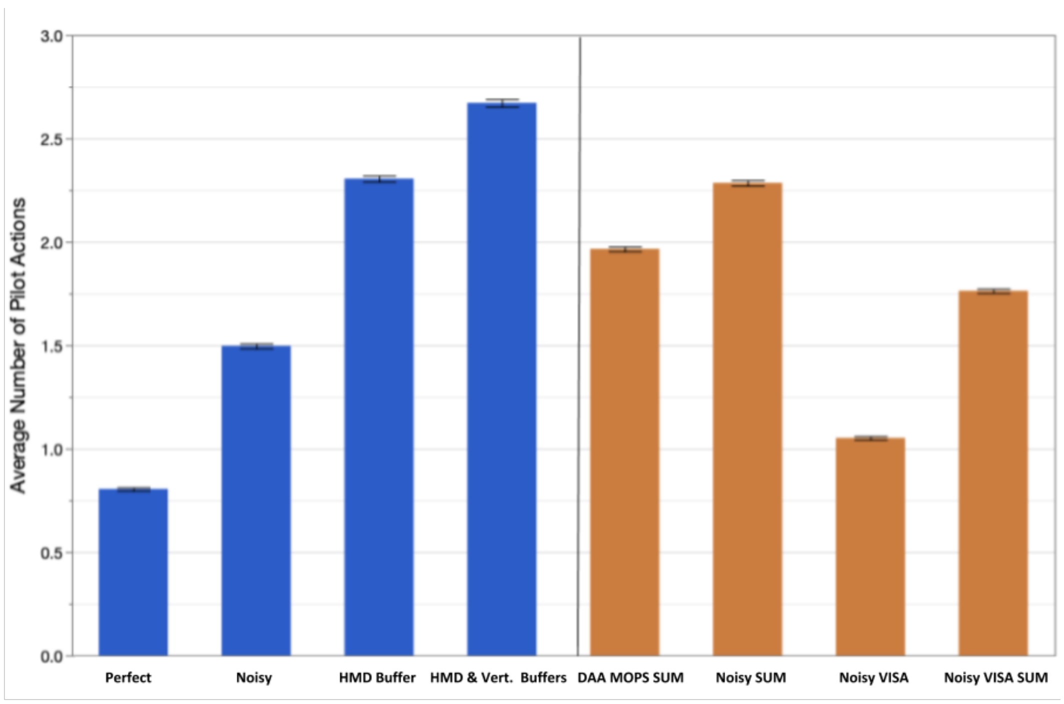

Figure 10: Best SUM and VISA Configurations: Pilot Workload N_{pa}

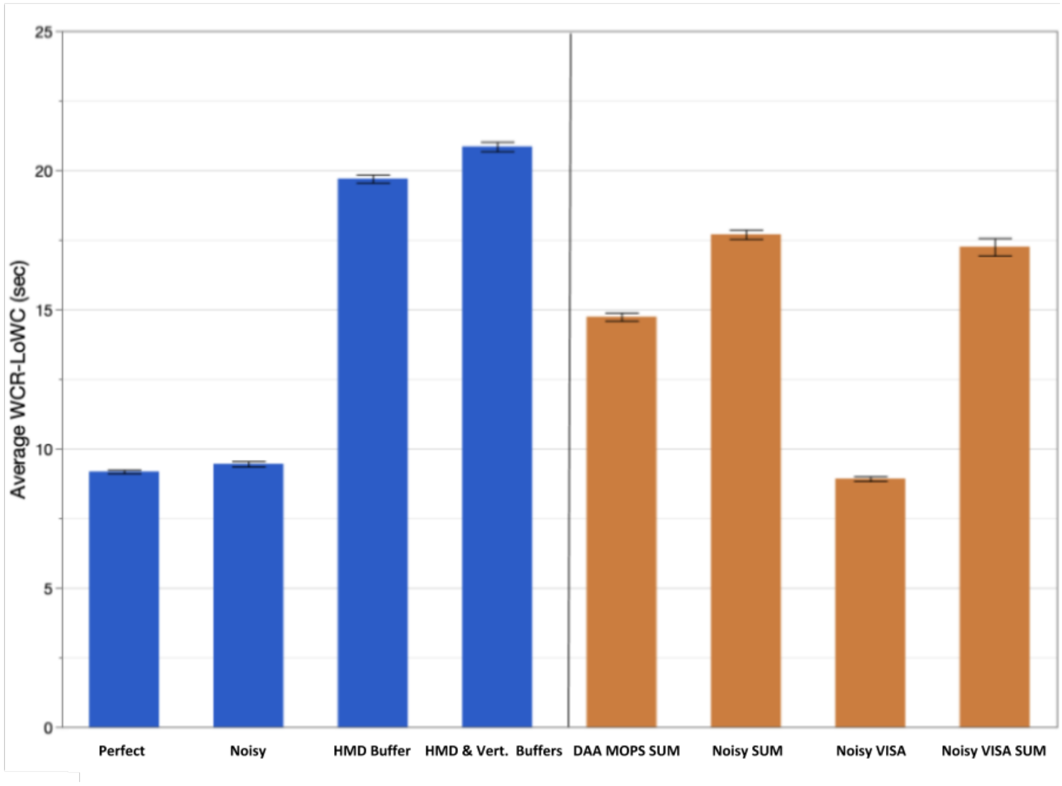

Figure 11: Best SUM and VISA Configurations: $t_{\text{WCR-LoDWC}}$

LoWC Severity ratio, with the best "Noisy SUM" configuration being only marginally better than "DAA MOPS SUM." VISA combined with DAIDALUS SUM in "Noisy VISA SUM" configuration achieved even better results. "HMD & Vert. buffer" yields the best results in this metric, slightly better than "Noisy VISA SUM." It is noteworthy that three of mitigated configurations, "HMD & Vert. buffer," "Noisy SUM," and "Noisy VISA SUM," have even lower SLoWC than the unmitigated "Perfect" configuration. This can be attributed to the fact that these configurations result in more conservative alerting and guidance that can better protect from maneuvering intruders. Therefore, it is not surprising that this advantage in LoWC severity Ratio metric is achieved at the cost of the second metric discussed in the next paragraph.

For the pilot workload metric (Figure 10), "Noisy VISA" was the only configuration that reduced the number of pilot actions against the unmitigated "Noisy" configuration. "Noisy VISA SUM" configuration was less effective in this metric, but still it outperformed all noisy configurations that did not use VISA. This is understandable since the main effect of VISA is the reduction of noise in intruder tracks processed by DAIDALUS, leading to more stable guidance. "Noisy SUM" configuration was found to be less effective in this metric than "DAA MOPS SUM." Note that "HMD & Vert. buffer" performed worse than all other configurations in this metric, while for LoWC severity Ratio metric it was the best.

Figure 11 compared WCR-to-LoDWC metric for different configurations and demonstrates trends similar to Figure 10. More importantly, the values of $t_{\text{WCR-LoDWC}}$ remain below acceptable 20 second limit for all four SUM and VISA combinations.

The combined performance index S for each configuration is shown in Figure 12. Note that, as

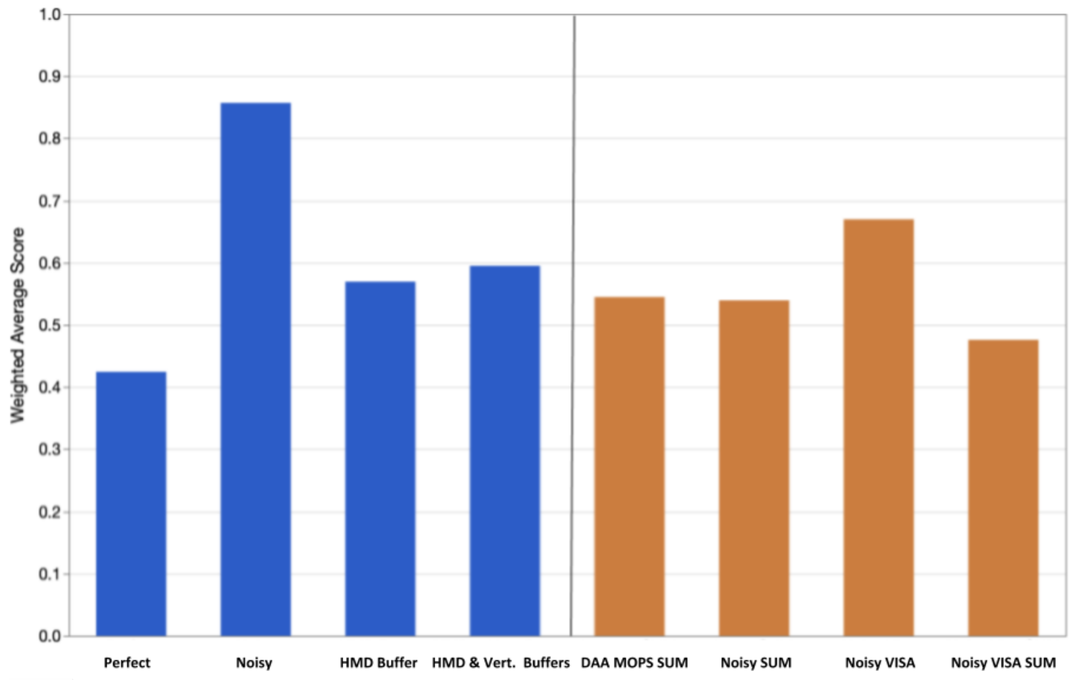

Figure 12: Best SUM and VISA Configurations: Weighted Average Score

for each individual metric, the lower values indicate the better overall performance. When all three metrics are taken into account, the differences in performance between different sensor uncertainty mitigation methods appear less pronounced than for each individual metric. In particular, VISA, even when it was used without SUM ("Noisy VISA" configuration), reduced S for "Noisy" configuration by 22%, comparable with 30% to 38% reduction achieved by other noise mitigation methods that did not involve VISA. Both "DAA MOPS SUM" and "Noisy SUM" configurations performed better than "Noisy VISA" and both buffered configurations, with "Noisy SUM" being marginally better. Of all compared noisy configurations, "Noisy VISA SUM" demonstrated the best overall performance, reducing S for "Noisy" configuration by 44%. This was achieved by modest improvements in the SLoWC ratio and $t_{\text{WCR-LoDWC}}$metrics and by more than 20% reduction in N_{pa} against the results of the Noisy SUM run.

6 Summary and Concluding Remarks

Sensor uncertainties may impact the performance of Detect-and-Avoid (DAA) systems. This paper evaluated the effectiveness of two static buffers, the Sensor Uncertainty Mitigation (SUM) scheme implemented in the Detect and Avoid Alerting Logic for Unmanned Systems (DAIDALUS), and the Virtual Intruder State Aggregation (VISA) method. Analysis focused on encounters involving unmanned aircraft with speeds between 40 and 110 KTAS flying below 11000 feet and non-cooperative aircraft with speeds below 170 KTAS detected by an airborne radar. Both open-loop simulations without aircraft maneuvers and closed-loop simulations involving a UAS pilot response model were performed on more than 80,000 encounters.

Three metrics were defined and computed for evaluating the effectiveness of horizontal and vertical buffers and DAIDALUS SUM in mitigating the impact of sensor noise. Results show a trade space between safety and operational suitability metrics. It was determined that DAIDALUS SUM performance was the best for a horizontal z_score equal to 2, or two standard deviations for horizontal position and velocity uncertainty, and it was relatively insensitive to vertical z_score parameters. However, this SUM configuration was only marginally better than "DAA MOPS SUM" configuration that was used in Appendix G of [26].

Configurations with static buffers achieved comparable performance. Note that a sensitivity study of the static buffer size was not conducted, so it is possible that using static buffers of different size can achieve even better results.

Interestingly, VISA, one of the simplest multi-state noise mitigation methods, was found to be almost as effective as other methods even when it was used without SUM and static buffers. Combining VISA with DAIDALUS SUM achieved even better performance than each mitigation method alone when used with DAIDALUS.

These results were found to be robust with respect to the choice of encounter data set. The results of this study may inform RTCA SC-228 in terms of validating sensor uncertainty requirements in the Phase 2 DAA MOPS and provide supporting data to the FAA's system safety assessment.

Acknowledgments

The authors want to express gratitude to Eric Wahl for his help in running simulations, and the whole DAA team at NASA for all fruitful discussions, help, and support.

References

1. *Code of Federal Regulation, General Operating and Flight Rules, title 14, sec. 91.113.* United States Department of Transportation: United States Federal Aviation Administration.

2. *Introduction to TCAS II Version 7.1.* United States Department of Transportation: United States Federal Aviation Administration, Washington, DC, 2011.

3. *Integration of Civil Unmanned Aircraft Systems (UAS) in the National Airspace System (NAS) Roadmap.* Federal Aviation Administration, Washington, DC, second edition, July 2018.

4. M. Abramson, M. Refai, and C. Santiago. The Generic Resolution Advisor and Conflict Evaluator (GRACE) for Unmanned Aircraft Detect-And-Avoid Systems. Technical Report NASA/TM-2017-219507, NASA Ames Research Center, Moffett Field, California, 2017.

5. M. Abramson, M. Refai, M. G. Wu, and S. Lee. Applying sensor uncertainty mitigation schemes to detect-and-avoid systems. In *2020 AIAA SciTech Forum and Exposition*. AIAA, June 2020.

6. M.S. Arulampalam, S. Maskell, N. Gordon, and T. Clapp. A tutorial on particle filters for online nonlinear/non-gaussian Bayesian tracking. In *Proceedings of IEEE Transactions on Signal Processing*, volume 50, pages 174–188. IEEE, 2002.

7. S. Ayyalasomayajula, F. Wieland, A. Trani, and N. Hinze. Unmanned aircraft system demand generation and airspace performance impact prediction. In *Proceedings of the 32nd IEEE Digital Avionics Systems Conference*, Syracuse, NY, 2013. IEEE.

8. V. L. Bageshwar and E. A. Euteneuer. Multi-intruder aircraft, multi-sensor tracking system. In *Proceedings of the 34th Digital AvionicsSystems Conference (DASC)*, pages 5A5–1–13, Prague, Czech Republic, 2015. IEEE/AIAA.

9. J. P. Chryssanthacopoulos and M. J. Kochenderfer. Accounting for state uncertainty in collision avoidance. In *Journal of Guidance, Control and Dynamics*, volume 34, pages 951–960. AIAA, 2011.

10. J. T. Davies and M. G. Wu. Comparative Analysis of ACAS-Xu and DAIDALUS Detect-and-Avoid Systems. Technical Report NASA/TM–2018–219773, NASA Ames Research Center, Moffett Field, California, 2018.

11. R. W. Ghatas, D. P. Jack, D. Tsakpinis, M. J. Vincent, J. L. Sturdy, C. A. Munoz, K. D. Hoffler, A. M. Dutle, R. R. Myer, A. M. DeHaven, E. T. Lewis, and K. E. Arthur. Unmanned aircraft systems minimum operational performance standards end-to-end verification and validation (e2-v2) simulation. Technical Report NASA/TM-2017-219598, NASA Langley Research Center, Hampton, VA, 2017.

12. R. W. Ghatas, D. Tsakpinis, J. L. Sturdy, D. P. Jack, R. R. Myer, and A. M. DeHaven. The effects of severity of losses of well clear on minimum operations performance standards end-to-end verification and validation simulation study for integrating unmanned aircraft systems into the national airspace system using detect and avoid systems. In *Proceedings of the 2018 AIAA Information Systems-AIAA Infotech @ Aerospace*, Kissimmee, FL, 2018. AIAA.

13. C. Hue, J.-P. Le Cadre, and P. Perez. Sequential Monte Carlo methods for multiple target tracking and data fusion. In *Proceedings of IEEE Transactions on Signal Processing*, volume 50, pages 309–325. IEEE, 2002.

14. D. P. Jack, K. D. Hoffler, and J. L. Sturdy. Mitigating the impact of sensor uncertainty on unmanned aircraft operations. Technical Report NASA CR 2017, NASA Langley Research Center, Hampton, VA, 2017.

15. M. Johnson, E. R. Mueller, and C. Santiago. Characteristics of a well clear definition and alerting criteria for encounters between uas and manned aircraft in class e airspace. In *Proceedings of the Eleventh USA/Europe Air Traffic Management Research and Development Seminar (ATM2015)*, Lisbon, Portugal, 2015.

16. P. R. Kalata. The tracking index: A generalized parameter for $\alpha - \beta$ and $\alpha - \beta - \gamma$ target trackers. In *Proceedings of IEEE Transactions on Aerospace and Electronic Systems*, volume AES-20, pages 174–182. IEEE, 1984.

17. M. J. Kochenderfer, J. K. Kuchar, L. P. Espindle, and J. Griffith. Uncorrelated encounter model of the national airspace system, version 1.0. Technical Report ATC-345, MIT Lincoln Laboratory, Lexington, Massachusetts, 2008.

18. P. Del Moral. Non linear filtering: Interacting particle solution. In *Markov Processes and Related Fields*, volume 2, page 555–580, 1996.

19. C. Muñoz, A. Narkawicz, G. Hagen, J. Upchurch, A. Dutle, and M. Consiglio. DAIDALUS: Detect and Avoid Alerting Logic for Unmanned Systems. In *Proceedings of the 34th Digital Avionics Systems Conference*, Prague, Czech Republic, 2015. IEEE/AIAA.

20. A. Narkawicz, C. Muñoz, and A. Dutle. Sensor Uncertainty Mitigation and Dynamic Well Clear Volumes in DAIDALUS. In *Proceedings of the 37th Digital Avionics Systems Conference*, London, UK, 2018. IEEE.

21. W. Olson. ACAS Xu UAS Detect and Avoid Solution. In *Proceedings of Lincoln Laboratory Air Traffic Control Workshop 2016 - 2*, number RTCA Paper No.261-15/PMC1400, 2016.

22. C. Park, H. Lee, and B. Musaffar. Radar data tracking using minimum spanning tree-based clustering algorithm. In *Proceedings of 11th AIAA Aviation Technology, Integration, and Operations (ATIO) Conference*, Virginia Beach, VA, 2011. AIAA.

23. P. Rohal and J. Ochodnicky. Radar target tracking by Kalman and particle filter. In *Proceedings of 2017 Communication and Information Technologies (KIT)*, Vysoke Tatry, Slovakia, 2017. IEEE.

24. SC-228. *Minimum Operational Performance Standards (MOPS) for Air-to-Air Radar for Traffic Surveillance (DO-366).* RTCA, Washington, DC, May 2017.

25. SC-228. *Minimum Operational Performance Standards (MOPS) for Detect and Avoid (DAA) Systems (DO-365).* RTCA, Washington, DC, May 2017.

26. SC-228. *Minimum Operational Performance Standards (MOPS) for Detect and Avoid (DAA) Systems (DO-365B).* RTCA, Washington, DC, 2020.

27. E. Theunissen, B. Suarez, and K. Kirk. Development, Integration and Testing of a Stand-Alone CDTI with Conflict Probing Support. In *Proceedings of the AIAA Infotech Aerospace Conference*, Garden Grove, California, June 2012. AIAA.

28. A. J. Weinert, E. P. Harkleroad, J. Grith, M. W. Edwards, and M. J. Kochenderfer. Uncorrelated Encounter Model of the National Airspace System, Version 2.0. Technical Report ATC-404, MIT Lincoln Laboratory, Lexington, Massachusetts, 2013.

29. M. G. Wu and S. Lee. Impact of Sensor Uncertainties on Detect-and-Avoid Systems' Separation Performance. In *2020 AIAA Aviation Forum*, Reno, NV (In Press), June 2020. AIAA.

30. M. G. Wu, S. Lee, and A. C. Cone. Detect and avoid alerting performance with limited surveillance volume for non-cooperative aircraft. In *AIAA Scitech 2019 Forum*, AIAA-2019-2073, 2019.

31. C. Yang, A. Mohammadi, and QW. Chen. Multi-sensor fusion with interaction multiple model and chi-square test tolerant filter. In *Sensors (Basel)*, volume 16. PMC, 2016.

32. P. Zarchan and H. Musoff. *Fundamentals of Kalman Filtering: A Practical Approach*, volume 190. AIAA, 2000.

33. F. Zhou, D. Zhou, and G. Yu. Target tracking in interference environments reinforcement learning and design for cognitive radar soft processing. In *Proceedings of 2008 Congress on Image and Signal Processing*, Sanya, Hainan, China, 2008. IEEE.

34. M. A. Zulkifley and B. Moran. Robust hierarchical multiple hypothesis tracker for multiple-object tracking. In *Expert Systems with Applications*, volume 39, pages 12319–12331, 2012.